Journal of Zhejiang University-SCIENCE B (Biomedicine & Biotechnology)
ISSN 1673-1581 (Print); ISSN 1862-1783 (Online)
www.jzus.zju.edu.cn; www.springerlink.com
E-mail: jzus@zju.edu.cn

Poly(D,L-lactic-*co*-glycolic acid)-based artesunate nanoparticles: formulation, antimalarial and toxicity assessments

Kabiru DAUDA[1], Zulaikha BUSARI[1], Olajumoke MORENIKEJI[1], Funmilayo AFOLAYAN[1], Oyetunde OYEYEMI[†‡2,3], Jairam MEENA[3], Debasis SAHU[3], Amulya PANDA[3]

([1]*Department of Zoology, University of Ibadan, Ibadan 200284, Nigeria*)

([2]*Department of Basic Sciences (Biology Programme), Babcock University, Ilishan-Remo 121103, Nigeria*)

([3]*Product Development Cell, National Institute of Immunology, Aruna Asaf Ali Marg, New Delhi 110067, India*)

[†]E-mail: zootund@yahoo.com; oyeyemio@babcock.edu.ng

Received Sept. 5, 2016; Revision accepted Dec. 14, 2016; Crosschecked Oct. 20, 2017

Abstract: Objective: The aim of this study was to formulate polymer-based artesunate nanoparticles for malaria treatment. Methods: Artesunate was loaded with poly(D,L-lactic-*co*-glycolic acid) (PLGA) by solvent evaporation from an oil-in-water single emulsion. Nanoparticles were characterized by X-ray diffraction and differential scanning calorimetry analyses. In vivo antimalarial studies at 4 mg/kg were performed on Swiss male albino mice infected with *Plasmodium berghei*. Hematological and hepatic toxicity assays were performed. In vitro cytotoxicity of free and encapsulated artesunate (Art-PLGA) to cell line RAW 264.7 was determined at concentrations of 7.8–1000 μg/ml. Results: The particle size of the formulated drug was (329.3±21.7) nm and the entrapment efficiency was (38.4±10.1)%. Art-PLGA nanoparticles showed higher parasite suppression (62.6%) compared to free artesunate (58.2%, P<0.05). Platelet counts were significantly higher in controls (305 000.00±148 492.40) than in mice treated with free artesunate (139 500.00±20 506.10) or Art-PLGA (163 500.00±3535.53) (P<0.05). There was no sign of hepatic toxicity following use of the tested drugs. The half maximal inhibitory concentration (IC_{50}) of Art-PLGA (468.0 μg/ml) was significantly higher (P<0.05) than that of free artesunate (7.3 μg/ml) in the in vitro cytotoxicity assay. Conclusions: A simple treatment of PLGA-entrapped artesunate nanoparticles with dual advantages of low toxicity and better antiplasmodial efficacy has been developed.

Key words: Poly(D,L-lactic-*co*-glycolic acid) (PLGA); Artesunate-PLGA delivery system; Antiplasmodial; Toxicity
http://dx.doi.org/10.1631/jzus.B1600389 **CLC number:** R978.61

1 Introduction

Malaria is a life threatening disease, which has attracted significant attention in terms of developing or improving drug regimens. The problems of toxicity and poor bio-distribution of most of the mainstay drugs for most parasitic diseases have necessitated the search for better alternatives. Artesunate, a partially synthetic derivative of artemisinin, has been approved for the treatment of malaria and has also been extensively documented for its anticancer properties (Woerdenbag *et al.*, 1993; Efferth, 2007; Liu *et al.*, 2011). Despite the therapeutic uses of artesunate, it has the disadvantage of a short half-life, therefore requiring frequent administration (Chadha *et al.*, 2012; Nguyen *et al.*, 2015). Its instability often causes easy degradation, resulting in poor pharmacokinetics and low bioavailability and pharmacological activity (Agnihotri *et al.*, 2013; Meng *et al.*, 2014). Therefore, development of a carrier that can maintain a sustained release profile and avoid rapid degradation of the drug is essential for its effective therapeutic usage.

The high bioavailability, good encapsulation, controlled release, and low toxicity of biodegradable

‡ Corresponding author
ORCID: Kabiru DAUDA, http://orcid.org/0000-0002-3089-2578

nanoparticles have resulted in their frequent use as drug delivery vehicles (Nguyen *et al.*, 2015). Poly(D,L-lactic-*co*-glycolic acid) (PLGA) is one of the most successful biodegradable polymers used for the development of nanoparticle treatments. Its hydrolysis within the body produces glycolic acid, which is a non-toxic biodegradable metabolite monomer (Kumari *et al.*, 2010). Along with approval for use in humans by the US Food and Drug Administration (Jain, 2000), this polymer is a good candidate for preparation of drug delivery systems for diseases like cancer, schistosomiasis, malaria, and other infectious agents (Mainardes and Evangelista, 2005; Acharya and Sahoo, 2011; Pradhan *et al.*, 2013; Nguyen *et al.*, 2015). While polymeric particle delivery of artesunate has undeniably enjoyed wide therapeutic application, its antimalarial potency and toxicological effects have not been studied.

Therefore, the aim of this study was to develop a polymeric drug delivery system for artesunate that has proper physical properties for improved malaria therapy and low toxicity.

2 Materials and methods

2.1 Materials

Artesunate (from *Artemisia annua* L. (Asteraceae)), polyvinyl alcohol (PVA; M_W=30–70 kDa), D-mannitol, dimethyl sulfoxide (DMSO), and 3-(4,5-dimethylthiazolyl-2)-2,5-diphenyltetrazolium bromide (MTT) were purchased from Sigma-Aldrich (St. Louis, MO, USA). PLGA (intrinsic viscosity η=0.41 dl/g, copolymer ratio 50:50, 45 kDa) was purchased from Purac Biochem, the Netherlands. Dichloromethane and acetone were procured from Merck Serono Ltd., Middlesex, UK. Water was purified using a Milli-Q_{plus} system from Millipore (MQ water, Ontario, Canada). Culture medium RPMI-1640, fetal calf serum (FCS), and antibiotic-antimycotic were obtained from GIBCO Invitrogen (Grand Island, NY, USA). All other chemicals were of analytical grade.

2.2 Preparation of nanoparticles

Artesunate-loaded PLGA (Art-PLGA) nanoparticles were formulated by solvent evaporation from an oil-in-water single emulsion (Chittasupho *et al.*, 2009). Briefly, 5 mg of artesunate was added to the organic phase containing 50 mg of polymer dissolved in 3.5 ml of dichloromethane and 0.5 ml of acetone to constitute a 1:10 (drug to polymer, w/w) ratio. The organic phase was then added drop-wise to 16 ml aqueous solution (2% PVA as emulsifier) with sonication using a sonicator (Qsonica sonicators, Newtown, USA) at 30 W with a 40% duty cycle for 3 min in ice-cold water. The emulsion was continuously stirred by magnetic stirrer (Thermo Scientific, Massachusetts, USA) at 300 r/min for 6 h to evaporate the solvent, leaving behind a colloidal suspension of the drug-encapsulated nanoparticles in aqueous phase. The formulation was centrifuged at 16000 r/min for 15 min using an ultracentrifuge (Beckman Coulter, Atlanta, USA) and then washed three times with MQ water. Dry powders were obtained by lyophilization of frozen samples in a freeze dryer (Labconco FreeZone 2.5, Kansas City, USA) in the presence of 5% mannitol as a cryoprotectant.

2.3 Measurement of particle size and zeta potential

The particle diameter, zeta potential, and polydispersity index (PDI) of the Art-PLGA-entrapped nanoparticulate drug were measured by a dynamic light scattering method using a Zetasizer Nano-ZS system (Malvern Instruments, UK). A homogenous solution obtained from dispersal of an appropriate amount of the formulated particle in MQ water was transferred to a clear disposable sizing cuvette for size and PDI measurements. A clear zeta cell was used for zeta potential analysis. Readings were taken in triplicate and results were expressed as mean±standard deviation (SD).

2.4 X-ray diffraction analysis and differential scanning calorimetry

X-ray diffraction (XRD) analysis was conducted on lyophilized Art-PLGA nanoparticles using an X'Pert-Pro multipurpose X-ray diffractometer (PANalytical, the Netherlands). The CuKα radiation was generated at 45 kV and 40 mA in the diffraction angle (2θ) range of 5°–40°.

Differential scanning calorimetry (DSC) was conducted on Art-PLGA nanoparticles to characterize the physical state of the drug. Thermograms were obtained using a Pyris 1 differential scanning calorimeter (PerkinElmer, USA). Dry nitrogen gas was used to purge the DSC cell at a flow rate of 40 ml/min.

About 6–8 mg of the formulation was sealed in a standard aluminum pan with a lid and heated at a rate of 5 °C/min from 50 °C to 300 °C.

2.5 Drug entrapment and encapsulation efficiency

Drug entrapment and encapsulation efficiency were determined using a modified form of the method described by Anitha *et al.* (2011). Lyophilized drug-loaded nanoparticles (10 mg) were dissolved in 1 ml acetonitrile (a common solvent for polymeric particles and drugs). The solution was thoroughly mixed and subjected to solvent evaporation for 9–10 h at 50 °C using a heater (CH-100, Biosan Ltd., Cambridge, UK). The residue was resuspended in 500 μl methanol, vortexed and centrifuged at 13000 r/min for 20 min. The supernatant (500 μl) was collected and stored. The process was repeated with 500 μl of acetonitrile.

A stock solution (1000 μg/ml) of artesunate was prepared by dissolving 5 mg of the drug in methanol (5 ml). The drug concentration of non-entrapped artesunate was determined using an ultraviolet-visible (UV-vis) spectrophotometer (Ultrospec 2100 pro, Amersham Biosciences, USA) at λ_{max} of 222 nm. Calibration plots of UV-vis spectrophotometer analysis of non-entrapped drug were obtained at concentrations ranging from 5 to 70 μg/ml. The supernatant containing encapsulated drug was analyzed by the same method. Then the drug content and encapsulation efficiency of the formulation were estimated.

2.6 Murine model and parasite strain

In vivo assays adhered to the Principles of Laboratory Animal Care (National Research Council, 2010). Swiss male albino mice were obtained from the Animal House Centre of the Department of Pharmacology, University of Ibadan, Nigeria. The rodent malaria line used was *Plasmodium berghei* NK-65 obtained from the Institute of Advanced Medical Research and Training (IAMRAT), University College Hospital, University of Ibadan, Nigeria.

2.7 Animals and conditions

A total of 15 Swiss male albino mice ((20.0±2.0) g) of 5–6 weeks old were used in a Peters' 4-d suppressive test on three groups with five mice each group. Animals were maintained in standard pathogen-free conditions and fed ad libitum.

2.8 Antiplasmodial evaluation using the Peters' 4-d suppressive test

On Day 0, *P. berghei*-infected erythrocytes (pEry) were obtained from an infected donor Swiss male mouse and diluted in physiological saline to 1×10^7 pEry/ml. Mice were infected intraperitoneally (ip) with an aliquot of 0.2 ml of the parasite suspension. The lyophilized Art-PLGA-entrapped nanoparticles were reconstituted in distilled water containing 10% Tween 80. At 2 h post-infection, the mice were treated orally with 0.1 ml of the nanoparticulate drug suspension with an equivalent artesunate composition of 4 mg/kg of body weight (Chinaeke *et al.*, 2015). The positive control group was treated orally with free artesunate at a dose of 4 mg/kg. The negative control group received 0.2 ml of the vehicle. On Days 1–3 post-infection, the Day 0 treatments were repeated in the experimental groups of mice. On Day 4 post-infection, blood smears prepared from the tail vein were Giemsa-stained and examined microscopically (Cheesbrough, 1998). The percentage parasitemia was determined microscopically by counting the number of infected erythrocytes among total erythrocytes in four fields of view. The percentage suppression of *P. berghei* was evaluated on the 4th day after treatment using the formula: $(A-B)/A\times100\%$, where A is the mean parasitemia in the untreated group (negative control) and B is the mean parasitemia in each treated group (Tona *et al.*, 2001). Animals were monitored daily for clinical signs and weight loss.

2.9 Rectal temperature and changes in weight

The rectal temperature and body weight of the mice and their baseline mean parasitemia before treatment were measured. The same measurements were repeated 4 d post treatment with free artesunate or the PLGA-encapsulated artesunate nanoparticulate drug.

2.10 Hematological and hepatic toxicity assays

Acclimatized albino rats (weight 94–105 g) were administered with drugs at similar concentrations to those used for the antiplasmodial study (i.e. 4 mg/kg for free and nano-formulated artesunate) for 4 d. Blood samples (2 ml) were collected from the rats through a retro-orbital puncture, into ethylene diamine tetraacetic acid (EDTA) tubes. Hematological parameters including packed cell volume (PCV), red

blood cell (RBC) count, white blood cell (WBC) count, neutrophils, eosinophils and hemoglobin (Hb) levels were evaluated in accordance with standard procedures. The cyanomethemoglobin method was used for the measurement of Hb levels; a hemocytometer was used to estimate the RBC and WBC counts, while PCV was measured by the conventional method of filling capillary tubes with blood and centrifuging using a microhematocrit centrifuge. The concentrations of plasma enzymes like aspartate aminotransferase (AST), alanine aminotransferase (ALT), and alkaline phosphate (ALP) were determined using Randox diagnostic kits.

2.11 Cell lines and culture

Murine RAW 264.7 macrophages were obtained from Product Development Cell-1 (National Institute of Immunology, New Delhi, India). The equilibrated cells were incubated in RPMI-1640 (Sigma, St. Louis, MO, USA) containing 10% FCS and 1% penicillin G/streptomycin/amphotericin B (PSA) at 37 °C and 5% CO_2 in an air humidified incubator. Cells were harvested when confluence was reached, and were washed with RPMI medium. The cells were diluted to 5×10^4 cells/ml with 200 μl of the cell suspension seeded per well in sterile 96-well plates and incubated for 24 h to allow cell attachment.

2.12 In vitro cell viability

The method of Zhang and Feng (2006) was adopted with some modifications. Briefly, the seeded RAW 264.7 cells (density, 5×10^4 viable cells/well) were incubated with free drug or the drug-loaded PLGA nanoparticle suspension at concentrations ranging from 7.8 to 1000 μg/ml for 24 h. At designated time intervals, the medium was removed and 100 μl of culture medium and 10 μl of MTT (5 mg/ml in phosphate-buffered saline (PBS)) were added to the wells. After incubation for 3–4 h, the culture solution was removed, leaving the precipitate of formazan crystals. DMSO (100 μl) was then added to each well before the plate was analyzed by a microplate reader at 570 nm. Cell viability was calculated using the following equation:

$$\text{Cell viability (\%)}=\text{Abs}_s/\text{Abs}_{control}\times100\%,$$

where Abs_s is the absorbance of the cells incubated with the PLGA-loaded nanoparticle suspension, and $\text{Abs}_{control}$ is the absorbance of the control containing cells incubated with the culture medium only. IC_{50} is the concentration at which the free drug or nanoparticle-entrapped drug inhibits cell growth by 50%, and is calculated using GraphPad Prism 6 statistical software (GraphPad Software Inc., La Jolla, CA, USA).

2.13 Statistical analysis

Data were entered in an MS-Excel spreadsheet and transferred to GraphPad Prism 6 (GraphPad Software Inc., La Jolla, CA, USA) for analysis. Two-way analysis of variance (ANOVA) and Tukey's multiple comparison tests were used to test for significant differences. A P-value of <0.05 was considered to be statistically significant. Cytotoxicity was expressed as the mean inhibition relative to the unexposed control±SD for three parallel readings.

3 Results

3.1 Characterization of nanoparticles

The size, PDI, and zeta potential of Art-PLGA-entrapped nanoparticles were (329.3±21.7) nm, 0.355±0.04, and (−17.4±7.1) mV, respectively. The drug entrapment efficiency (%EE) was (38.4±10.1)%. The effects of surfactants and drug/polymer ratios on nanoparticle characteristics are presented in Table 1.

The crystalline contents of the formulated nanoparticles were determined by powder X-ray diffraction (P-XRD) analysis. The P-XRD diffractograms for

Table 1 Effects of surfactants and drug/polymer ratios on nanoparticle characteristics

Surfactant	OP:EAP	Drug:PLGA	Particle size (nm)*	Zeta potential (mV)*	PDI*
1% PVA	1:5 (4 ml:20 ml)	□:5 (10 mg:50 mg)	3330.00±1.88	−13.3±3.3	0.869±0.094
2% SLS	1:4 (4 ml:16 ml)	1:10 (2.5 mg:25 mg)	340.60±5.15	−14.1±3.9	0.322±0.124
2% PVA	1:5 (4 ml:20 ml)	1:5 (10 mg:50 mg)	7300.00±1.70	−24.5±12.4	1.000±0.000
2% PVA	1:4 (4 ml:16 ml)	1:10 (5 mg:50 mg)	329.30±21.70	−17.4±7.1	0.355±0.040
1% SLS	1:4 (4 ml:16 ml)	1:10 (5 mg:50 mg)	3700.00±0.60	−16.6±22.5	0.653±0.122

*Data are expressed as mean±SD (n=3); OP: organic phase; EAP: external aqueous phase; PVA: polyvinyl alcohol; SLS: sodium lauryl sulfate; PDI: polydispersity index

Art-PLGA showed two peaks representing 2θ of 42.1° and 43.7°, respectively (Fig. 1). The DSC thermogram of PLGA-entrapped artesunate showed no intensive endothermic peak for artesunate. However, a sharp PLGA relaxation peak at 47 °C was observed along with a diminished PLGA glass transition peak from 55 °C to 65 °C (Fig. 2). A very weak thermal event was present between 140 °C and 150 °C. Intensive endothermic events occurred from 260 °C to 300 °C.

3.2 Parasite suppression

The percentage parasite suppression was lower (58.2%) in the free artesunate group than in the group treated with the nano-synthesized form (62.6%) at 4 d post-treatment. No parasite reduction was observed in the control group (Table 2).

3.3 Variation in body weight and rectal temperature

The body weight of mice decreased from (28.0±3.2) g on Day 0 to (26.0±1.3) g on Day 4 after treatment with free artesunate, and from (24.2±3.2) g to (23.2±1.2) g in the control group during the same period (P>0.05). However, there was a weight gain from (28.2±2.7) g to (29.2±1.7) g in mice treated with the Art-PLGA nanoparticulate drug (P>0.05) (Table 2). There was a significant temperature gain from (34.5±1.0) °C to (36.8±1.0) °C in mice treated with free artesunate and from (33.7±0.4) °C to (36.2±0.9) °C in mice treated with Art-PLGA nanoparticulate drugs (P<0.05) (Table 2). No temperature gain was observed in the control group.

3.4 Variation in hematological and liver function parameters

There was no significant variation in most of the observed hematological parameters in free or nano-formulated artesunate exposed groups compared with the control group (P>0.05). However, the platelet counts (305 000.00±148 492.40) observed in the control group were significantly higher than those in the free (139 500.00±20 506.10) and nano-formulated drug (163 500.00±3535.53) treatment groups (Table 3). There were no significant differences in AST or ALT concentrations in all experimented groups, whereas the ALP concentration was significantly lower in the free artesunate group ((70.5±19.1) U/L) than in the control ((120.5±6.4) U/L) and the nano-synthesised groups ((110.5±4.9) U/L) (P<0.05; Fig. 3).

3.5 In vitro cell viability

Art-PLGA nanoparticles showed lower toxicity than the free drug. Cell viability data following treatment with free artesunate or Art-PLGA-entrapped nanoparticles are presented in Fig. 4. Cell viability varied in a concentration-dependent manner (P<0.001). Generally, cells became less viable at higher doses.

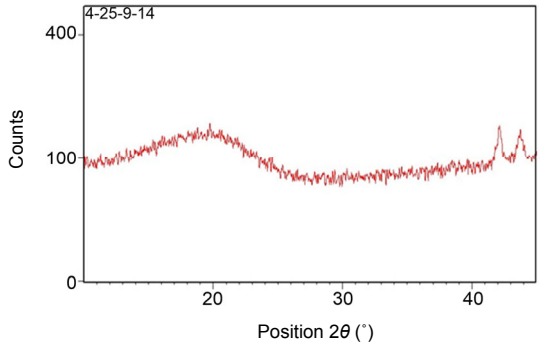

Fig. 1 XRD spectra of formulated polymeric nanoparticles

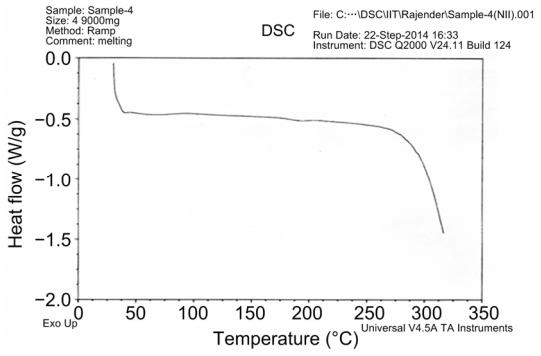

Fig. 2 Thermogram of Art-PLGA nanoparticles

Table 2 Response to treatment in Swiss albino mice

Group	Parasitemia*	Parasite suppression (%)	Weight (g)*			Temperature (°C)*		
			Before	After	P	Before	After	P
Art-free	1.9±0.7[a]	58.2	28.0±3.2	26.0±1.3	>0.05	34.5±1.0	36.8±1.0	<0.05
Art-PLGA	1.7±0.1[a]	62.6	28.2±2.7	29.2±1.7	>0.05	33.7±0.4	36.2±0.9	<0.05
Control	4.5±0.6[b]		24.2±3.2	23.2±1.2	>0.05	36.1±0.5	36.3±1.0	>0.05

Similar superscript letters in the same column denote no significant difference while different letters denote a significant difference. Parasitemia denotes mean of parasite counts in 5 mice representing each experimental group. * Data are expressed as mean±SD (n=5)

The IC_{50} of Art-PLGA (468.0 μg/ml) was significantly higher than that of free artesunate (7.3 μg/ml).

4 Discussion

The method employed in the formulation yielded particles which appeared soluble and finely dispersed in water when compared to the free non-entrapped drugs. Dry lyophilized nanoparticles have been shown to have good physical and chemical stability and can be stored at room temperature for over 6 months without decomposition or aggregation (Bhawana *et al.*, 2011). The influence of the larger surface area of nanoparticles in promoting dissolution has been emphasized (McNeil, 2005). The negative zeta potential denotes non-toxicity and the values for all formulations fall within the acceptable range for easy charge neutralization, thus favoring less interference in in vivo studies (Nordström, 2011). The PDI of our formulation, which was less than 0.4, will enhance moderate distribution (Nobbmann, 2014). The nanoparticles could, however, be further optimised to give a narrow range of monodispersed PDI for better drug distribution. The mean Art-PLGA nanoparticle size ((329.3±21.7) nm) observed in our study was larger than that found in a related study ((289.6±4.6) nm) (Nguyen *et al.*, 2015). Our formulation also showed lower drug entrapment efficiency ((38.4±10.1)%) than that shown in that study ((42.36±0.73)%). The PLGA concentration, volume of the aqueous phase, and type of surfactants and stability agents used are known to affect particle size, PDI, and encapsulation efficiency (Wohlfart *et al.*, 2011; Cooper and Harirforoosh, 2014). An increase in aqueous phase volume produces small nanoemulsion droplets, which decrease the size and PDI of the particles while an increase in PLGA concentration increases the viscosity of the polymer solution, resulting in poorer dispersibility of the organic phase in the aqueous phase (Nguyen *et al.*, 2015).

The diffractogram patterns showing peaks at 42.1° and 43.7° 2θ suggest the amorphous nature of Art-PLGA (Panda *et al.*, 2016). The absence of a decomposition exotherm indicates the increased physical stability of the drug in the formulation (Chadha *et al.*, 2012). The thermogram of the Art-PLGA nanoparticles, which did not show any intensive endothermic peaks, indicates that chemical interactions which could alter the drug or the polymer

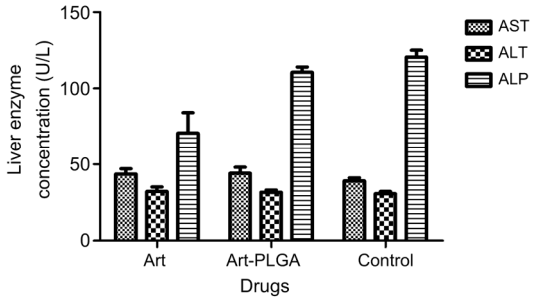

Fig. 3 Hepatic toxicity assessment of free and nanoparticulate artesunate

AST: aminotransferase; ALT: alanine aminotransferase; ALP: alkaline phosphate; Art: artesunate; Art-PLGA: artesunate entrapped PLGA nanoparticles. Data are expressed as mean±SD (n=5)

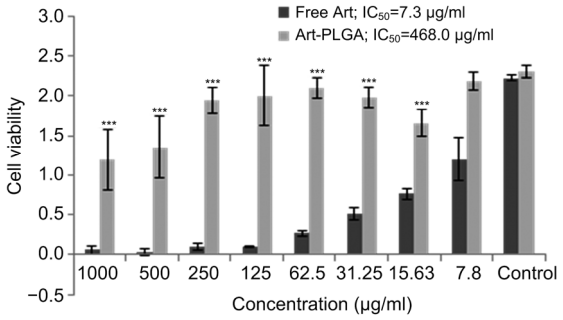

Fig. 4 Cell viability and inhibitory concentrations in free and entrapped drugs

IC_{50}: half maximal inhibitory concentration; Art: artesunate; Art-PLGA: artesunate-entrapped PLGA nanoparticles. Data are expressed as mean±SD (n=3). *** P<0.001, vs. free Art

Table 3 Hematological variation between free and nano-synthesised artesunate treatments

Group	PCV (%)	Hb (g/dl)	RBC ($\times10^6$/cm^3)	WBC ($\times10^3$/cm^3)	Platelet ($\times10^3$/cm^3)	Lymphocyte (%)	Neutrophil (%)	Monocyte (%)
Artesunate	37.00±2.83^a	12.20±0.92^a	5.80±0.61^a	6.10±1.17^a	139.50±20.51^a	64.00±2.83^a	31.50±3.54^a	2.50±0.71^a
Art-PLGA	37.50±2.12^a	12.00±0.57^a	6.20±0.08^a	8.80±2.47^a	163.50±3.54^a	70.00±0.00^a	26.50±0.71^a	1.50±0.71^a
Control	37.00±2.83^a	12.10±0.78^a	5.70±0.59^a	12.00±8.94^a	305.00±148.49^b	63.50±2.12^a	32.00±1.41^a	2.00±1.41^a

Similar superscript letters in the same column denote no significant difference while different letters denote a significant difference. PCV: packed cell volume; Hb: hemoglobin; RBC: red blood cell; WBC: white blood cell. Data are expressed as mean±SD (n=5)

properties did not occur during particle formulation (Panda *et al.*, 2016). However, the presence of endothermic events at 260–300 °C could be due to residual excipients or the presence of impurities in the drug or polymer. It is also possible that polymers are corrosive in nature and their melting and interaction with the metal pan in previous samples may have resulted in the generation of peaks in non-specific regions. The very weak thermal event between 140 °C and 150 °C could have been due to the melting of artesunate. However, in the Art-PLGA formulation, the amount of artesunate was small compared to that in PLGA, and hence no significant endotherm was visible.

The increase in suppression of *P. berghei* in Art-PLGA-treated mice compared with those in the free drug and control groups was consistent with the findings of a report on the antimalarial properties of artesunate-loaded solid lipid microparticles, in which improved activity was linked to the drug's sustained release action (Chinaeke *et al.*, 2015). There was no parasite suppression in the control group since no drug was administered. The *P. berghei* murine model has been widely adopted for systematic screening of potential antimalarial drugs at the early stages of drug discovery. The screening results, however, do not always translate to the occurrence of *Plasmodium falciparum* malaria in man. Thus, there is a need to perform similar studies in a *P. falciparum* animal model (Ibrahim *et al.*, 2014). The efficacy of Art-PLGA nanoparticles may be related to their ability to penetrate mucus and microvilli barriers. Nanoparticles as large as 500 nm encapsulated with a mucoinert polymer have been observed to traverse physiological human mucus rapidly, with diffusivities only 4-fold lower than their rates in pure water (Lai *et al.*, 2007). The capacity of the polymeric nanoparticles to protect the encapsulated drug and its stability in the digestive tract have been reported to facilitate improved cellular uptake and controlled drug release at the target (des Rieux *et al.*, 2006).

The negative association between *P. berghei* parasitemia and rectal temperature as observed in free artesunate and Art-PLGA-treated groups was consistent with earlier reports (Dikasso *et al.*, 2006; Chinaeke *et al.*, 2015). While weight loss in the control group could be associated with parasite burden, the loss of weight in the group treated with free artesunate could also result from toxic effects of the drug. There were no significant differences in most of the observed hematological parameters between mice administered with free artesunate or Art-PLGA nanoparticles and the control groups. However, the significantly lower platelet counts in the treated groups compared with the control group were consistent with the claim that the best side effect of artemisinin-based compounds is that they lower reticulocyte counts (Clark, 2012). Artesunate's interaction with erythrocyte plasma membranes initiates a reaction between the drug and ferrous iron in the heme prosthetic group of hemoglobin, thus activating the drug to form toxic free radicals (Clark, 2012). The mechanism of action of artesunate and its ability to accumulate in the erythrocytes are associated with hemotoxicity (Bigoniya *et al.*, 2015). The controlled release of artesunate from PLGA, however, could have resulted in the higher reticulocyte counts compared with the free drug. The lack of significant differences in transaminases, the important markers of hepatocellular toxicity and damage (Faber *et al.*, 1981), suggests that free and nanoparticulate drugs are not toxic to the liver at the tested concentrations.

With the growing evidence of artesunate-associated toxicity to normal cells or tissues (Mesembe *et al.*, 2004; White *et al.*, 2006) and poor delivery, our method of polymer encapsulation of artesunate with reduced toxicity and effective delivery to target cells becomes more promising. The results of the in vitro cytotoxicity assay on the RAW 264.7 cell line further support the safety of PLGA nanoparticulate artesunate compared with the free drug.

A simple formulation of PLGA-entrapped artesunate nanoparticles with dual advantages of low toxicity and better antiplasmodial efficacy has been developed. The formulated nanoparticulate drugs will augment research efforts towards developing antimalarial drugs with enhanced delivery and efficacy.

Acknowledgements

Oyetunde OYEYEMI acknowledges the Centre for Science and Technology of the Non-Aligned and Other Developing Countries (NAM S&T Centre) in collaboration with the Department of Science & Technology (DST), the Government of India for "Research Training Fellowship for Developing Country Scientists (RTF-DCS)" award, undertaken at the National Institute of Immunology, New Delhi, India.

Compliance with ethics guidelines

Kabiru DAUDA, Zulaikha BUSARI, Olajumoke MORENIKEJI, Funmilayo AFOLAYAN, Oyetunde OYEYEMI, Jairam MEENA, Debasis SAHU, and Amulya PANDA declare that they have no conflict of interest.

All institutional and national guidelines for the care and use of laboratory animals were followed.

References

Acharya, S., Sahoo, S.K., 2011. PLGA nanoparticles containing various anticancer agents and tumour delivery by EPR effect. *Adv. Drug Del. Rev.*, **63**(3):170-183. http://dx.doi.org/10.1016/j.addr.2010.10.008

Agnihotri, J., Singh, S., Bigonia, P., 2013. Formal chemical stability analysis and solubility analysis of artesunate and hydroxychloroquinine for development of parenteral dosage form. *J. Pharm. Res.*, **6**:117-122. http://dx.doi.org/10.1016/j.jopr.2012.11.025

Anitha, A., Deepagan, V.G., Rani, V.V.D., *et al*., 2011. Preparation, characterization, in vitro drug release and biological studies of curcumin loaded dextran sulphate-chitosan nanoparticles. *Carbohyd. Poly.*, **84**(3):1158-1164. http://dx.doi.org/10.1016/j.carbpol.2011.01.005

Bhawana, R.K., Basniwal, H.S., Buttal, V.K., *et al*., 2011. Curcumin nanoparticles: preparation, characterization, and antimicrobial study. *J. Agric. Food Chem.*, **59**(5): 2056-2061. http://dx.doi.org/10.1021/jf104402t

Bigoniya, P., Sahu, T., Tiwari, V., 2015. Hematological and biochemical effects of sub-chronic artesunate exposure in rats. *Toxicol. Rep.*, **2**:280-288. http://dx.doi.org/10.1016/j.toxrep.2015.01.007

Chadha, R., Gupta, S., Pathak, N., 2012. Artesunate-loaded chitosan/lecithin nanoparticles: preparation, characterization, and in vivo studies. *Drug Dev. Ind. Pharm.*, **38**(12):1538-1546. http://dx.doi.org/10.3109/03639045.2012.658812

Cheesbrough, M., 1998. District Laboratory Practice in Tropical Countries. Part 1. Cambridge University Press, London.

Chinaeke, E.E., Chime, S.A., Onyishi, V.I., *et al.*, 2015. Formulation development and evaluation of the anti-malaria properties of sustained release artesunate-loaded solid lipid microparticles based on phytolipids. *Drug Deliv.*, **22**(5):652-665. http://dx.doi.org/10.3109/10717544.2014.881633

Chittasupho, C., Xie, S.X., Baoum, A., *et al.*, 2009. ICAM-1 targeting of doxorubicinloaded PLGA nanoparticles to lung epithelial cells. *Eur. J. Pharm. Sci.*, **37**(2):141-150. http://dx.doi.org/10.1016/j.ejps.2009.02.008

Clark, R.L., 2012. Effects of artemisinins on reticulocyte counts and and relationship to possible embryotoxicity in confirmed and unconfirmed malarial patients. *Birth Def. Res. Part A: Clin. Mol. Teratol.*, **94**(2):61-75. http://dx.doi.org/10.1002/bdra.22868

Cooper, D.L., Harirforoosh, S., 2014. Design and optimization of PLGA-based diclofenac loaded nanoparticles. *PLoS ONE*, **9**(1):e87326. http://dx.doi.org/10.1371/journal.pone.0087326

des Rieux, A., Fievez, V., Garinot, M., *et al.*, 2006. Nanoparticles as potential oral delivery systems of proteins and vaccines: a mechanistic approach. *J. Control Release*, **116**(1):1-27. http://dx.doi.org/10.1016/j.jconrel.2006.08.013

Dikasso, D., Makonnen, E., Debella, A., *et al.*, 2006. In vivo anti-malaria activity of hydroalcoholic extract from *Asparaginus africanus* in mice infected with *Plasmodium berghei*. *Ethiop. J. Health Dev.*, **20**(2):112-118. http://dx.doi.org/10.4314/ejhd.v20i2.10021

Efferth, T., 2007. Willmar Schwabe Award 2006: antiplasmodial and antitumor activity of artemisinin-from bench to bedside. *Planta Med.*, **73**(4):299-309. http://dx.doi.org/10.1055/s-2007-967138

Faber, J.L., Chein, K.R., Mitlnacht, S., 1981. Myocardial ischemia: the pathogenesis of irreversible cell injury in ischemia. *Am. J. Pathol.*, **102**(2):271-281.

Ibrahim, N., Ibrahim, H., Dormoi, J., *et al*., 2014. Albumin-bound nanoparticles of practically water-soluble antimalarial lead greatly enhance its efficacy. *Int. J. Pharm.*, **464**(1-2):214-224. http://dx.doi.org/10.1016/j.ijpharm.2014.01.001

Jain, R.A., 2000. The manufacturing techniques of various drug loaded biodegradable poly(lactide-*co*-glycolide) (PLGA) devices. *Biomaterials*, **21**(23):2475-2490. http://dx.doi.org/10.1016/S0142-9612(00)00115-0

Kumari, A., Yadav, S.K., Yadav, S.C., 2010. Biodegradable polymeric nanoparticles based drug delivery systems. *Coll. Surf. B: Biointer.*, **75**(1):1-18. http://dx.doi.org/10.1016/j.colsurfb.2009.09.001

Lai, S.K., O'Hanlon, D.E., Harrold, S., *et al.*, 2007. Rapid transport of large polymeric nanoparticles in fresh undiluted human mucus. *Proc. Natl. Acad. Sci. USA*, **104**(5): 1482-1487. http://dx.doi.org/10.1073/pnas.0608611104

Liu, W.M., Gravett, A.M., Dalgleish, A.G., 2011. The antimalarial agent artesunate possesses anticancer properties that can be enhanced by combination strategies. *Int. J. Cancer*, **128**(6):1471-1480. http://dx.doi.org/10.1002/ijc.25707

Mainardes, R.M., Evangelista, R.C., 2005. PLGA nanoparticles containing praziquantel effect of formulation variables on size distribution. *Int. J. Pharm.*, **290**(1-2):137-144. http://dx.doi.org/10.1016/j.ijpharm.2004.11.027

McNeil, S.E., 2005. Nanotechnology for the biologist. *J. Leuk. Biol.*, **78**(3):585-592. http://dx.doi.org/10.1189/jlb.0205074

Meng, H., Xu, K., Xu, Y., *et al.*, 2014. Nanocapsules based on mPEGylated artesunate prodrug and its cytotoxicity. *Coll. Surf. B: Biointer.*, **115**:164-169. http://dx.doi.org/10.1016/j.colsurfb.2013.11.039

Mesembe, O.E., Ivang, A.E., Udo-Attah, G., *et al.*, 2004. A morphometric study of the teratogenic effect of artesunate

on the central nervous system of the Wistar rats foetus. *Nig. J. Physiol. Sci.*, **19**(1):92-97.

National Research Council, 2010. Guide for the Care and Use of Laboratory Animals. National Academies Press, Washington, DC.

Nguyen, H.T., Tran, T.H., Kim, J.O., *et al.*, 2015. Enhancing the in vitro anti-cancer efficacy of artesunate by loading into poly D,L-lactide-*co*-glycolide (PLGA) nanoparticles. *Arch. Pharm. Res.*, **38**(5):716-724. http://dx.doi.org/10.1007/s12272-014-0424-3

Nobbmann, U.L.F., 2014. Polydispersity—what does it mean for DLS and chromatography? http://www.materials-talks.com/blog/2014/10/23/polydispersity-what-does-it-mean-for-dls-and-chromatography [accessed on Oct. 24, 2016]

Nordström, P., 2011. Formulation of Polymeric Nanoparticles Encapsulating and Releasing a New Hydrophobic Cancer Drug. MS Thesis, Chalmers University of Technology, Göteborg, Sweden.

Panda, A., Meena, J., Katara, R., *et al*., 2016. Formulation and characterization of clozapine and risperidone co-entrapped spray-dried PLGA nanoparticles. *Pharm. Dev. Technol.*, **21**(1):43-53. http://dx.doi.org/10.3109/10837450.2014.965324

Pradhan, R., Poudel, B.K., Ramasamy, T., *et al.*, 2013. Docetaxel loaded polylactic acid-*co*-glycolic acid nanoparticles: formulation, physicochemical characterization and cytotoxicity studies. *J. Nanosci. Nanotechnol.*, **13**(8):5948-5956. http://dx.doi.org/10.1166/jnn.2013.7735

Tona, L., Mesia, K., Ngimbi, N.P., *et al.*, 2001. In vivo antimalarial activity of *Cassia occindentalis*, *Morinda morindoides* and *Phyllanthus niruri*. *Ann. Trop. Med. Parasitol*., **95**(1):47-57. http://dx.doi.org/10.1080/00034983.2001.11813614

White, T.E., Bushdid, P.B., Ritter, S., *et al.*, 2006. Artesunate-induced depletion of embryonic erythroblasts precedes embryolethality and teratogenicity in vivo. *Birth Def. Res. Part B*: *Dev. Reprod. Toxicol.*, **77**(5):413-429. http://dx.doi.org/10.1002/bdrb.20092

Woerdenbag, H.J., Moskal, T.A., Pras, N., *et al.*, 1993. Cytotoxicity of artemisinin-related endoperoxides to Ehrlich ascites tumor cells. *J. Nat. Prod.*, **56**(6):849-856. http://dx.doi.org/10.1021/np50096a007

Wohlfart, S., Khalansky, A.S., Gelperina, S., *et al.*, 2011. Efficient chemotherapy of rat glioblastoma using doxorubicin-loaded PLGA nanoparticles with different stabilizers. *PLoS ONE*, **6**:e19121. http://dx.doi.org/10.1371/journal.pone.0019121

Zhang, Z.P., Feng, S.S., 2006. The drug encapsulation efficiency, in vitro drug release, cellular uptake and cytotoxicity of paclitaxel-loaded poly(lactide)-tocopheryl polyethylene glycol succinate nanoparticles. *Biomaterials*, **27**(21):4025-4033. http://dx.doi.org/10.1016/j.biomaterials.2006.03.006

中文概要

题　目：基于聚乳酸羟乙酸共聚物的青蒿琥酯纳米颗粒的制备，及其抗疟活性和毒性评价

目　的：为疟疾治疗制定基于聚合物的青蒿琥酯纳米粒。

创新点：以聚乳酸羟乙酸共聚物（PLGA）为载体，制备青蒿琥酯纳米颗粒。并以小鼠为模型，评估其抗疟疗效和安全性。

方　法：以 PLGA 为载体，采用从单一的水包油乳剂中进行溶剂蒸发的方法制备青蒿琥酯纳米颗粒。借助 X 射线衍射和差示扫描量热分析对纳米颗粒进行表征。以 4 mg/kg 的剂量对感染疟原虫的雄性瑞士白化小鼠进行体内抗疟活性的研究，测定血液和肝毒性的相关指标。体外实验以小鼠腹腔巨噬细胞细胞系 RAW 264.7 为模型，在 7.8~1000 μg/ml 浓度范围内，测定游离型和包裹型青蒿琥酯的细胞毒性。

结　论：实验结果表明，纳米颗粒的粒径为(329.3±21.7) nm，包封率为(38.4±10.1)%。与游离青蒿琥酯（58.2%）相比，基于 PLGA 的青蒿琥酯纳米颗粒（Art-PLGA）具有较高的抑虫率（62.6%），$P<0.05$。就血小板计数结果而言，对照组（305 000.00±148 492.40）明显地高于游离青蒿琥酯组（139 500.00±20 506.10）和 Art-PLGA 组（163 500.00±3535.53），$P<0.05$。因此，药物的使用没有导致肝毒性的产生。体外细胞毒性试验结果表明，Art-PLGA 的半数抑制浓度（IC_{50}，468.0 μg/ml）显著高于游离青蒿琥酯（7.3 μg/ml），$P<0.05$。基于 PLGA 的青蒿琥酯纳米颗粒是一种有效安全的抗疟治疗方法。

关键词：青蒿琥酯-PLGA 缓释系统；抗疟原虫；毒性